



New chiral pyridine-based Eu(III) complexes: Study of the relationship between the nature of the ligands and the 5D_0 luminescence spectra

Fabio Piccinelli^{a,*}, Adolfo Speghini^a, Magda Monari^b, Marco Bettinelli^a

^a Laboratorio di Chimica dello stato solido, DB, Univ. Verona and INSTM, Udr Verona, Strada Le Grazie 15, 37134 Verona, Italy

^b Dipartimento di Chimica "G. Ciamician", Università di Bologna, Via Selmi 2, 40126 Bologna, Italy

ARTICLE INFO

Article history:

Received 1 August 2011

Received in revised form 16 December 2011

Accepted 21 December 2011

Available online 12 January 2012

Keywords:

Europium

Luminescence

Crystal structure

Nitrogen ligands

Chirality

Nitrate compounds

ABSTRACT

In this paper a new family of imines [*N,N'*-bis(2-pyridylmethylidene)-1,2-(*R,S*)-cyclohexanediamine (ligand **1**); *N,N'*-bis(2-pyridylmethylidene)-1,2-(*R,S*)-cyclohexanediamine (ligand **3**)] and amines [*N,N'*-bis(2-pyridylmethylene)-1,2-(*R,R* + *S,S*)-cyclohexanediamine (ligand **2**); *N,N'*-bis(2-pyridylmethylene)-1,2-(*R,S*)-cyclohexanediamine (ligand **4**)] pyridine-based chiral ligands and their chiral nitrate Eu(III) complexes is presented. Combination of structural and spectroscopic evidences in the solid state, reveals that the Eu(III) ion environment is characterized by a low symmetry for all the complexes. The $^5D_0 \rightarrow ^7F_0$ Eu(III) emission intensity reflects the degree of distortion of the metal surroundings, that is higher in the case of *cis* isomer of amine-based complex. This new family of Eu(III) chiral complexes are promising candidates for applications in the sensing field as probes in solution of the nitrate anion and of chiral molecules.

© 2011 Elsevier B.V. All rights reserved.

1. Introduction

Luminescent lanthanide complexes have interesting photo-physical properties mainly due to the spectroscopic features of the metal ion. In particular, the emission spectra of lanthanide ions consist of sharp and narrow bands corresponding to the parity-forbidden *f*-*f* transitions that are characteristic of the metal ion. Among the most emissive lanthanide ions we mention the europium(III) which possesses [Xe]4f⁶ electronic configuration, 7F_0 as a ground state and 5D_0 long-lived excited state [1]. Some transitions have variable intensities resulting from the sensitivity to the structural details of the metal ion environment. It is well known that the $^5D_0 \rightarrow ^7F_2$ transition located around 615 nm is highly sensitive to the chemical environment and for this reason it is described as "hypersensitive". A particularly useful characteristic of the Eu(III) ion is the emission features of the $^5D_0 \rightarrow ^7F_0$ transition. Both the ground state and excited state are non-degenerate, which results, in principle, in a one-to-one correspondence between the number of peaks in the emission spectrum and the number of distinct Eu(III) ion environments [2–4]. Concerning the transition energy of the $^5D_0 \rightarrow ^7F_0$ emission, it is well known that this energy is strongly connected to the total charge on ligands coordinated to Eu(III) [2,4].

Although Ln(III) ions have weak absorption intensities, due to the parity forbidden nature of the intraconfigurational *f*-*f* transitions,

this disadvantage can be overcome by indirect sensitization through the absorption bands of the ligand molecules coordinated to the Ln(III) ion using UV light (antenna effect). Another advantage of the bond between Ln(III) ions and organic ligands is to allow the protection of the Ln(III) ions from external quenching processes such as the intrusion of solvent molecules (i.e. H₂O) into the inner sphere coordination of the metal ion. These molecules are responsible of the non-radiative deactivation processes that occur upon interaction with OH, NH, and CH oscillators present around the lanthanide ion.

Concerning the applications in the biomedical field, Eu(III) complexes exhibit some desirable and unusual characteristic when compared with conventional organic fluorophores such as long excited-state lifetime (in the ms-range), large shift between absorbed and emitted wavelength (in the case of ligand sensitization) and line-like emission bands these features allowing the separation between Ln(III) luminescence and short-lived background fluorescence [5]. Recently, the interest in Ln(III) compounds possessing chiral properties has started to increase because, in addition to the interesting spectral characteristics discussed above it is possible to take advantage of chiral features introduced in the design of the complex [6–9]. In particular, the availability of chiral Ln(III) compounds, where the chirality is "introduced" through the use of chiral ligands, has led to the development of new chiral sensing/recognition applications, such as luminescence sensing of anions [10,11] and of chiral biological substrates [11–13].

The major advantage of introducing chirality into luminescent Ln(III)-based complexes appears to be the enhancement of the

* Corresponding author.

E-mail address: fabio.piccinelli@univr.it (F. Piccinelli).

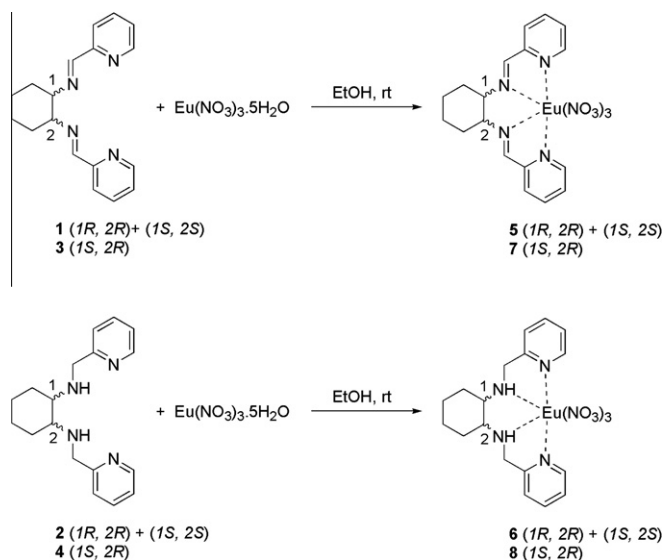


Fig. 1. Synthetic protocol employed for the synthesis of chiral nitrate Eu(III) complexes.

molecular recognition/sensing properties (i.e. sensitivity, specificity, selectivity, etc.) towards biological materials. In fact, the luminescent chiral complexes are amenable to be analyzed by CPL spectroscopy, that is strongly dependent on the chiral environment around the metal. For this reason, this technique is particularly suitable for investigating interactions with other chiral molecules [14].

In the present contribution we show a convenient synthetic protocol for the synthesis of a new family of tetradentate nitrogen chiral ligands and their chiral nitrate Eu(III) complexes. We have studied and analyzed the effects of the flexibility and stereochemistry of the ligand on the geometric environment of the Eu(III) ion, establishing a relationship with the emission features of the metal ion with the help, when possible, of the solid state molecular structure of the complexes. The emission spectra and the decay curves of solids **5–8** complexes (Fig. 1) upon direct laser excitation of

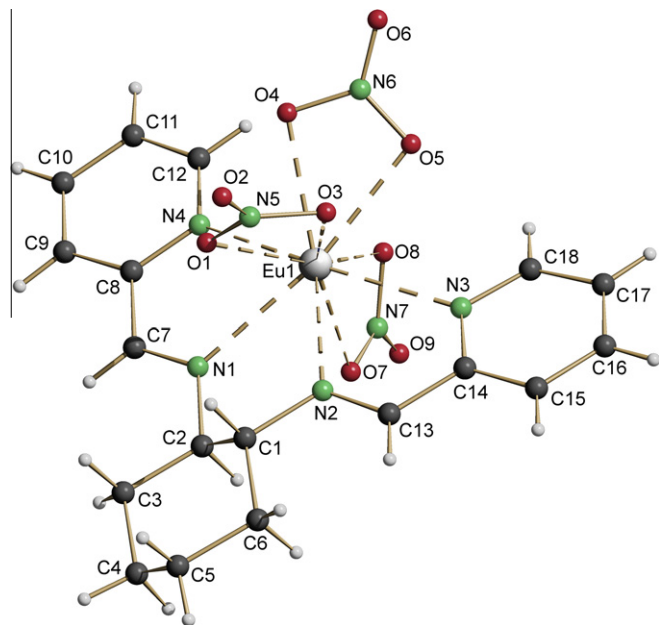


Fig. 2. Perspective view of complex **5**.

the Eu(III) ion (465 nm) were measured, and the crystal structure of **5** and **6** (Figs. 1 and 2) were determined.

2. Experimental

We performed the synthesis of *N,N'*-bis(2-pyridylmethylidene)-1,2-(*R,R* + *S,S*)-cyclohexanediamine (**1**) (racemic mixture) starting from (\pm)-*trans*-1,2-cyclohexanediamine, following the same synthetic protocol reported in the literature for the synthesis of the enantiopure form [15]. The same protocol was also employed for the synthesis of the ligand **3** (*N,N'*-bis(2-pyridylmethylidene)-1,2-(*R,S*)-cyclohexanediamine), starting from *cis*-1,2-cyclohexanediamine.

Ligand **3** was purified by precipitation from a cold (0 °C) diethyl ether solution. Chemical yield 72%, ¹H NMR (CD₃CN, 300 MHz): δ 8.61 (d, *J* 4 Hz, 2H), 8.33 (s, 2H), 7.95 (d, *J* 8 Hz, 2H), 7.78 (t; *J* 8 Hz, 2H), 7.38 (dd, *J* 4, 8 Hz, 2H), 3.73 (m, 2H), 2.05 (m, 4H), 1.77 (m, 2H), 1.63 (m, 2H) IR (KBr pellet, cm⁻¹): 3086, 3057, 3010, 2925, 2856, 1649, 1585, 1564, 1468, 1444, 1435, 1318, 1070, 1041, 981, 978, 966, 875, 787, 769, 740.

Ligand **2** [*N,N'*-bis(2-pyridylmethylene)-1,2-(*R,R* + *S,S*)-cyclohexanediamine]: 250 mg (0.85 mmol) of the ligand **1** were dissolved in 10 mL of methanol and at 0 °C, 155 mg (4.1 mmol) of NaBH₄ were added. The reaction mixture was left to reach room temperature and stirred for 3 h (the formation of the ligand **2** was checked by TLC (R_f = 0.4, DCM/MeOH = 99.5/0.5)). After that, 30 ml of distilled water were added to the reaction mixture and almost all methanol was evaporated under vacuum. The aqueous layer was extracted with 20 mL of DCM and the organic phase containing the ligand was separated and dried under anhydrous Na₂SO₄. The organic solvent was evaporated under vacuum and **2** (yield 92%) was collected as a pale yellow oil. ¹H NMR (CD₃CN, 300 MHz): δ 8.97 (d, *J* 4 Hz, 2H), 8.17 (dd, *J* 4, 8 Hz, 2H), 7.90 (d, *J* 8 Hz, 2H), 7.67 (t; *J* 8 Hz, 2H), 4.25 (d, *J* 12 Hz, 2H), 4.44 (d, *J* 12 Hz, 2H), 2.61 (m, 2H), 2.44 (m, 2H), 2.20 (m, 2H), 1.72 (m, 2H), 1.53 (m, 2H). IR (neat, cm⁻¹): 3292, 3062, 3008, 2923, 2852, 1591, 1570, 1473, 1448, 1433, 1354, 1255, 1146, 1119, 1047, 995, 858, 760.

Ligand **4** [*N,N'*-bis(2-pyridylmethylene)-1,2-(*R,S*)-cyclohexanediamine]: 205 mg (0.70 mmol) of the ligand **3** were dissolved in 10 mL of methanol and at 0 °C, 127 mg (3.37 mmol) of NaBH₄ were added. The reaction mixture was left to reach room temperature and stirred for 3 h (the formation of **4** was checked by TLC (R_f = 0.35, DCM/MeOH = 99.5/0.5)). After that, 30 ml of distilled water were added to the reaction mixture and almost all methanol was evaporated under vacuum. The aqueous layer was extracted with 20 mL of DCM and the organic phase containing the ligand was separated and dried under anhydrous Na₂SO₄. The organic solvent was evaporated under vacuum and **4** (yield 81%) was collected as a pale yellow oil. ¹H NMR (CD₃CN, 300 MHz): δ 8.47 (d, *J* 4 Hz, 2H), 7.79 (pt, *J* 8 Hz, 2H), 7.51 (d, *J* 8 Hz, 2H), 7.30 (dd, *J* 4, 8 Hz, 2H), 3.76 (d, *J* 16 Hz, 2H), 3.88 (d, *J* 16 Hz, 2H), 2.78 (m, 2H), 1.76 (m, 2H), 1.69 (m, 2H), 1.48 (m, 2H), 1.37 (m, 2H). IR (neat, cm⁻¹): 3317, 3058, 3008, 2929, 2852, 1591, 1570, 1473, 1457, 1435, 1373, 1342, 1300, 1223, 1147, 1047, 995, 758.

The synthesis of Eu(III) complexes was performed in absolute ethanol (20 mL), by adding 0.5 mmol of the ligand and 0.5 mmol of Eu(NO₃)₃·5H₂O (L:Eu = 1:1). The mixture was stirred for 3 h at room temperature and in all cases white powder insoluble in ethanol was collected. All powders were characterized by elemental analysis, IR spectroscopy and, when possible the molecular structure was determined by single-crystal X-ray diffraction.

Complex 5: Yield = 78%. Elemental Anal. Calc. for C₂₀H₂₃N₈O₉Eu (MW 671.411): C, 35.78; H, 3.45; N, 16.69; O, 21.45. Found: C, 35.73; H, 3.40; N, 16.73; O, 21.48%. IR (KBr pellet, cm⁻¹): 3105, 3072, 2943, 2856, 2252, 1651, 1595, 1479, 1385, 1350, 1311,

1284, 1157, 1028, 1011, 814, 783, 741, 636. Single crystals suitable for X-ray diffraction were obtained by slow evaporation of an acetonitrile solution of **5**.

Complex 6: Yield = 84%. Elemental Anal. Calc. for $C_{18}H_{24}N_7O_9Eu$ (MW 634.39): C, 34.08; H, 3.81; N, 15.46; O 22.70. Found: C, 34.06; H, 3.78; N, 15.49; O, 22.71%. IR (KBr pellet, cm^{-1}): 3257, 3093, 3068, 3035, 2945, 2926, 2862, 1608, 1572, 1520, 1462, 1371, 1319, 1302, 1161, 1038, 1014, 818, 769, 741. Single crystals suitable for X-ray diffraction were obtained by slow diffusion of diethyl ether in a solution of **6** in acetonitrile.

Complex 7: Yield = 85%. Elemental Anal. Calc. for $C_{18}H_{20}N_7O_9Eu$ (MW 630.358): C, 34.30; H, 3.20; N, 15.55; O 22.84. Found: C, 34.27; H, 3.16; N, 16.57; O, 22.86%. IR (KBr pellet, cm^{-1}): 3091, 3066, 2931, 2870, 1649, 1595, 1487, 1448, 1385, 1362, 1304, 1227, 1055, 1028, 1011, 989, 777, 739.

Complex 8: Yield = 92%. Elemental Anal. Calc. for $C_{18}H_{24}N_7O_9Eu$ (MW 634.39): C, 34.08; H, 3.81; N, 15.46; O, 22.70. Found: C, 34.05; H, 3.76; N, 15.47; O, 22.74%. IR (KBr pellet, cm^{-1}): 3284, 3107, 3070, 3037, 2976, 2945, 2924, 2858, 1608, 1572, 1495, 1435, 1385, 1317, 1290, 1155, 1045, 1034, 1003, 816, 764, 739.

Elemental analyses were carried out by using an EACE 1110 CHNOS analyzer.

2.1. Spectroscopic measurements

Luminescence measurements were carried out using a tunable dye laser pumped by a Nd:YAG laser. The emission signal was analyzed by a half-meter monochromator (HR460, Jobin Yvon) equipped with a 1200 lines/mm grating and detected with a CCD detector (Spectrum One, Jobin Yvon) or with a photomultiplier. The spectral resolution of the emission spectra is 0.1 nm. The emission decay curves were recorded upon pulsed laser excitation using a water cooled GaAs photomultiplier (Hamamatsu) and a 500 MHz digital oscilloscope (WaveRunner, LeCroy). The emission spectra of **5–8** complexes were recorded on powdered samples possessing the same crystal structure shown in Figs. 1 and 2 in the case of complex **5** and **6**.

2.2. X-ray structural determinations

The X-ray intensity data were measured on a Bruker SMART Apex II CCD area detector diffractometer for **5** and **6**. The cell dimensions and the orientation matrix were initially determined from a least-squares refinement on reflections measured in three sets of 20 exposures, collected in three different ω regions, and eventually refined against all data. For all crystals, a full sphere of reciprocal space was scanned by $0.3^\circ\omega$ steps. The software SMART [16] was used for collecting frames of data, indexing reflections and determination of lattice parameters. The collected frames were then processed for integration by the SAINT [16] program, and an empirical absorption correction was applied using SADABS [17]. The structures were solved by direct methods (SIR 97) [18] and subsequent Fourier syntheses and refined by full-matrix least-squares on F^2 (SHELXTL) [19], using anisotropic thermal parameters for all non-hydrogen atoms. Crystals of complex **5** showed the presence of one crystallization acetonitrile molecule in the asymmetric unit. In complex **6** two nitrate ligands were affected by disorder over two positions with occupation factors of 0.66 and 0.34 for the main and minor isomers, respectively. The kind of disorder is different in the two nitrates. In fact in one nitrate (N5) only the two chelating oxygens (O1b and O2b) are disordered over two sites and the second image results from a rotation of the planar nitrate [O1b, O2b, N5, O3] of $84.7(7)^\circ$ with respect to the main image [O1a, O1b, N5, O3] whereas for the second nitrate (N6) all four atoms give a distinct second image [N6b, O4b, O5b, O6b] which is rotated with respect to the first one [N6a, O4a, O5a, O6a]

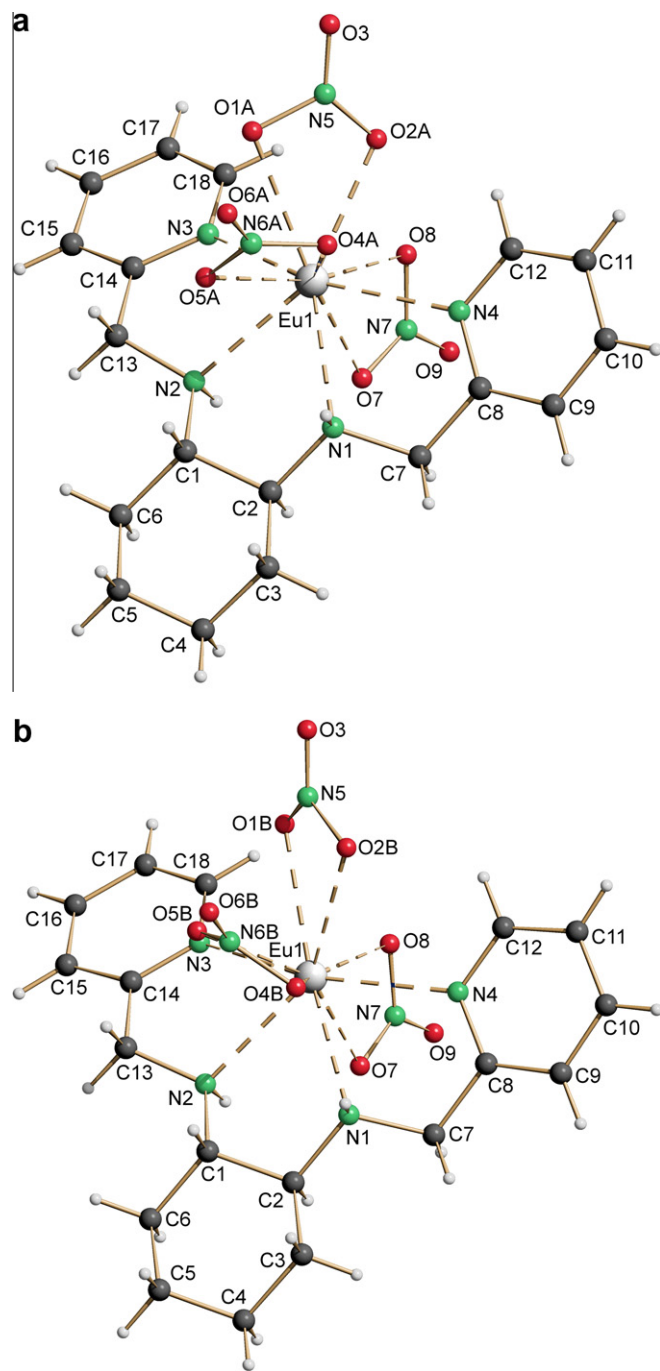


Fig. 3. (a) Dominant conformational isomer of complex **6** (occupation factor 0.66). (b) Minor conformational isomer of the complex **6** (occupation factor 0.34).

of $49.8(5)^\circ$ (please compare Fig. 3a and b). All hydrogen atoms, except the ones bound to nitrogens that were refined isotropically, were added in calculated positions, included in the final stage of refinement with isotropic thermal parameters, $U(H) = 1.2 U_{eq}(C)$ and allowed to ride on their carrier carbons. Crystal data and details of the data collection for all structures are reported in Table 1. Molecular graphics were generated using SCHAKAL [20].

3. Results and discussion

The synthetic protocol for the synthesis of the nitrate complexes studied in this paper is shown in Fig. 1.

Table 1
Crystal data and structure refinement for **5-CH₃CN** and **6**.

Compound	5-CH₃CN	6
Formula	C ₁₈ H ₂₀ EuN ₇ O ₉ ·CH ₃ CN	C ₁₈ H ₂₄ EuN ₇ O ₉
Formula weight	671.42	634.40
T (K)	293(2)	293(2)
λ (Å)	0.71073	0.71073
Crystal symmetry	monoclinic	orthorhombic
Space group	P2 ₁ /c	Pbca
a (Å)	9.7970(7)	12.8584(17)
b (Å)	16.2185(13)	14.5569(19)
c (Å)	16.5723(12)	25.434(3)
α (°)	90	90
β (°)	102.714(4)	90
γ (°)	90	90
Cell volume (Å ³)	2568.7(3)	4760.7(10)
Z	4	8
D _{calc} (Mg m ⁻³)	1.736	1.770
μ (Mo Kα) (mm ⁻¹)	2.506	2.697
F(000)	1336	2528
Crystal size (mm)	0.10 × 0.15 × 0.20	0.20 × 0.25 × 0.30
θ limits (°)	1.78–25.00	2.25–28.69
Reflections collected	21881	48669
Unique observed reflections	3661 [R _{int} = 0.0912]	5874 [R _{int} = 0.0682]
[F ₀ > 4σ(F ₀)]		
Goodness-of-fit (GOF) on F ²	0.979	1.035
R ₁ (F ²), wR ₂ (F ²) [I > 2σ(I)] ^b	0.0656, 0.1152	0.0478, 0.1244
Largest difference in peak and hole (e Å ⁻³)	1.219 and -1.215	1.307 and -1.742

^a $R_1 = \sum ||F_o| - |F_c|| / \sum |F_o|$.

^b $wR_2 = [\sum w(F_o^2 - F_c^2)^2 / \sum w(F_o^2)^2]^{1/2}$ where $w = 1/[\sigma^2(F_o^2) + (aP)^2 + bP]$ where $P = (F_o^2 + F_c^2)/3$.

As shown in this figure the 1 and 2 carbon stereocenters were systematically varied as well as the flexibility of the ligand structure. In fact, it is possible to increase the structural flexibility employing diamine-like ligands (**2** and **4**) instead of imine-like ones (**1** and **3**).

3.1. Structural studies of **5** and **6**

Complex **5** crystallizes in the centric space group P2₁/c and therefore the racemic mixture is present. In the asymmetric unit of the crystal of complex **5** one complex and one crystallization acetonitrile molecule are present. The Eu(III) ion has a 10-fold

Table 2
Selected bond lengths (Å) and angles (°) for complexes **5** and **6**.

Bond lengths for complex 5		Bond lengths for complex 6	
Eu(1)–N(1)	2.561(9)	Eu(1)–N(1)	2.575(4)
Eu(1)–N(2)	2.53(1)	Eu(1)–N(2)	2.544(4)
Eu(1)–N(3)	2.63(1)	Eu(1)–N(3)	2.584(5)
Eu(1)–N(4)	2.622(9)	Eu(1)–N(4)	2.560(4)
Eu(1)–O(1)	2.549(8)	Eu(1)–O(1A)	2.644(4)
Eu(1)–O(3)	2.539(9)	Eu(1)–O(1B)	2.60(2)
Eu(1)–O(4)	2.488(8)	Eu(1)–O(2A)	2.506(8)
Eu(1)–O(5)	2.496(8)	Eu(1)–O(2B)	2.624(5)
Eu(1)–O(7)	2.485(8)	Eu(1)–O(4A)	2.464(6)
Eu(1)–O(8)	2.465(8)	Eu(1)–O(4B)	2.56(1)
		Eu(1)–O(5A)	2.516(7)
		Eu(1)–O(5B)	2.57(1)
		Eu(1)–O(7)	2.470(4)
		Eu(1)–O(8)	2.531(4)
Bond angles for complex 5		Bond angles for complex 6	
N(1)–Eu(1)–N(2)	63.4(3)	N(1)–Eu(1)–N(2)	66.7(1)
N(1)–Eu(1)–N(3)	123.2(3)	N(1)–Eu(1)–N(3)	128.5(1)
N(1)–Eu(1)–N(4)	63.3(3)	N(1)–Eu(1)–N(4)	64.8(1)
N(2)–Eu(1)–N(3)	64.2(3)	N(2)–Eu(1)–N(3)	63.2(2)
N(2)–Eu(1)–N(4)	126.7(3)	N(2)–Eu(1)–N(4)	129.7(1)
N(3)–Eu(1)–N(4)	158.5(3)	N(3)–Eu(1)–N(4)	152.6(2)

Average bond lengths: for complex **5** Eu–N(av) 2.59 Å, Eu–O(av) 2.50 Å; for complex **6** Eu–N(av) 2.57 Å, Eu–O 2.52 Å (dominant conformational isomer) 2.56 Å (minor conformational isomer). Average N–Eu–N bite angles: for complex **5** 63.5°, for the two isomers of complex **6** 64.9°.

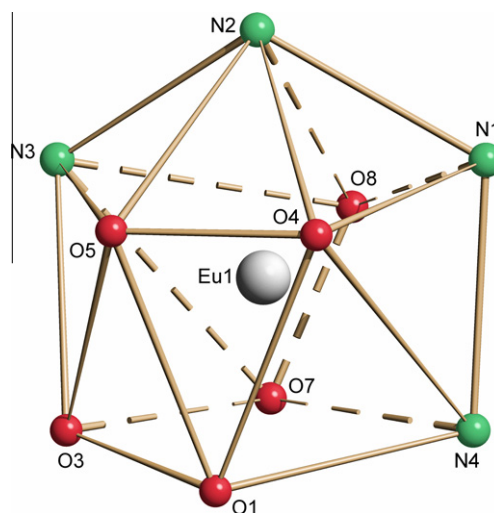


Fig. 4. Coordination polyhedron around the Eu(III) ion of complex **5**.

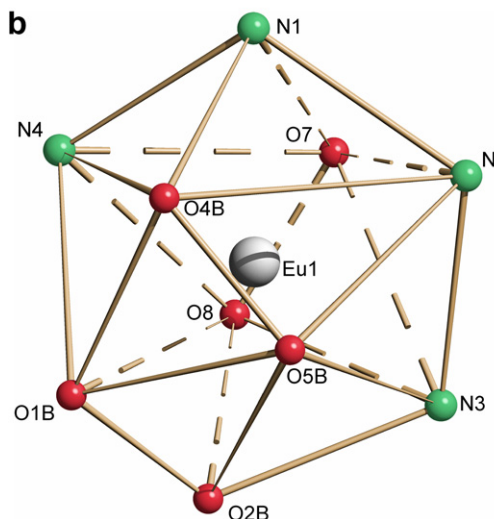
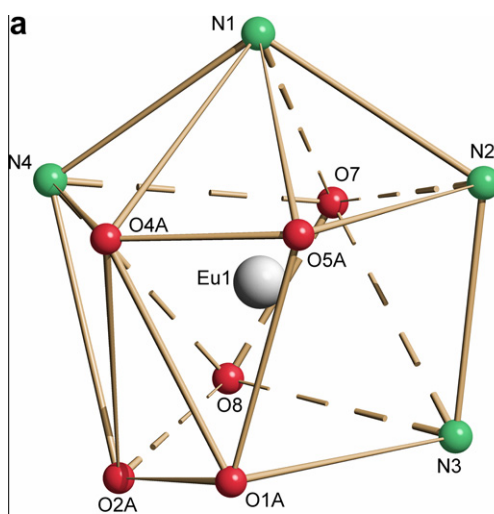


Fig. 5. Coordination polyhedra around the Eu(III) ion of the dominant (a) and the minor (b) conformational isomers of complex **6**.

coordination, being coordinated by one tetradentate ligand **1** and three bidentate nitrates (Fig. 2, selected bond lengths and angles in Table 2). The observed coordination polyhedron is a distorted

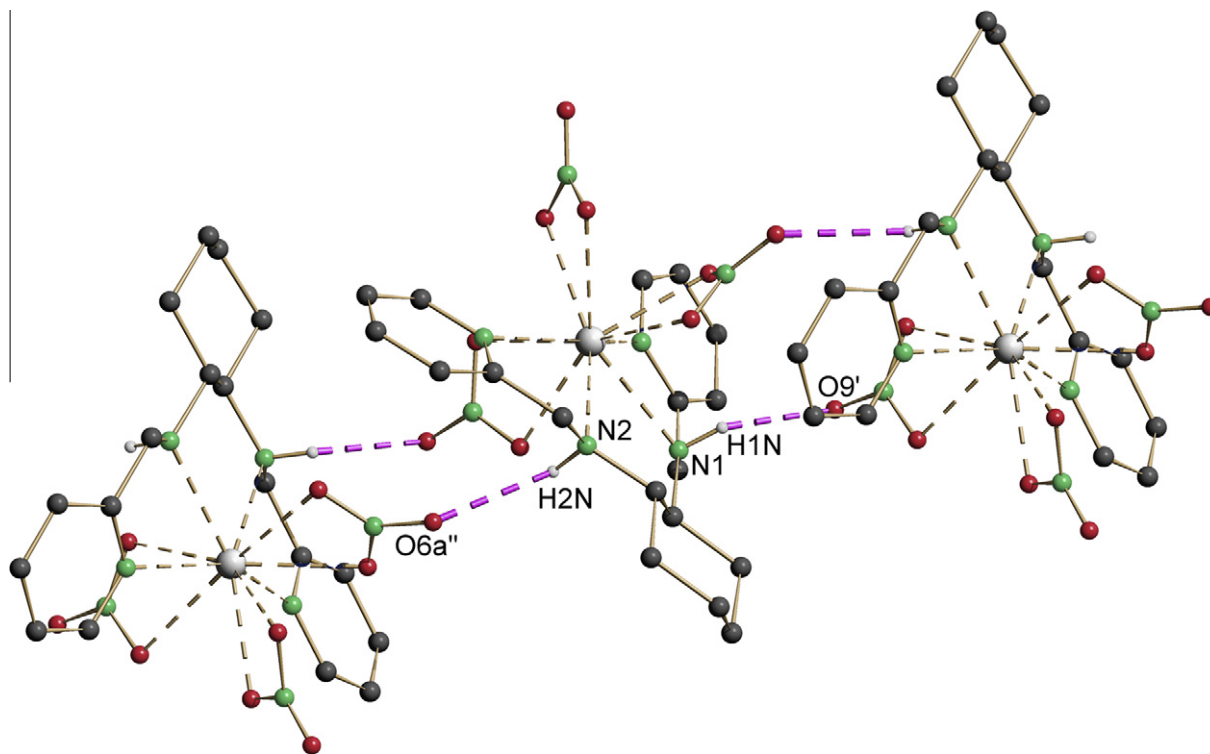


Fig. 6. Detail of the observed structural motif in the crystal packing of complex **6** (fragment of chain built by intermolecular hydrogen bonds). [N(1)–H(1N), 0.891(3) Å, N(1)–H(1N)···O9', 142.40(7)°; H(1N)···O9', 2.259(4) Å, N(1)···O(9'), 3.015(8) Å and N(2)–H(2N), 0.861(4) Å, N(2)–H(2N)···O6a'', 139.58(8)°; H(2N)···O6a'', 2.390(6) Å; N(2)···O(6a''), 3.096(4) Å]. [The primed atoms are generated by the symmetry operation: (') $-x + 3/2, y + 1/2, z$; (") $-x + 3/2, y - 1/2, z$] (All hydrogens not involved in H bonds are omitted for clarity).

sphenocorona (Fig. 4). The N atoms of the tetradentate ligand deviate from an ideal square planar geometry [N(1): +0.20(1) Å, N(2): –0.20(1) Å, N(3): 0.102(5) Å, N(4): –0.101(6) Å], and the distance of the Eu ion from the coordinating N atoms of the N_4 least square plane is 0.41(1) Å.

The crystal structure of complex **6** consists of discrete molecules of [Eu(2)(NO₃)₃]. Complex **6** crystallizes in the centric space group *Pbca* and therefore the racemic mixture is present. The Eu(III) ion is coordinated by one tetradentate ligand **2** and analogously to complex **5** three chelating nitrates give rise to 10-fold coordination at the metal ion (Fig. 3a and b). Two out of the three coordinated nitrates (N5 and N6) show disorder (see Section 2) only of the chelating oxygen atoms over two positions (N5) or an independent second image (N6) thus generating two conformational isomers characterized by different occupation factors (Fig. 3a and b) and generating different coordination polyhedra. In particular, we observe a sphenocorona and a bicapped square antiprism polyhedra [21], for the major and the minor conformational isomers, respectively (Fig. 5a and b). In both cases, due to the very low site symmetry (C_1) of the Eu(III) ion, the polyhedra are significantly distorted compared with the ideal geometry. It is worth to mention the presence of an axial distortion in the metal coordination environment of the major isomer of complex **6**. In fact, in comparison with the averaged Eu–O bond length (2.52 Å, Table 2), we observe two short Eu–O bonds for the almost antipodal O4a and O7 ligand atoms (i.e. Eu(1)–O(4a) 2.464(4) Å, Eu(1)–O(7) 2.470(4) Å, O(4a)–Eu(1)–O(7) 142.85(8)°, Table 1 and Fig. 5a). The distance of the Eu ion from the least square plane N_4 defined by the coordinating N atoms is 0.456(3) Å, and the deviations of the nitrogen atoms from the N_4 least square plane are less pronounced in comparison with those found in complex **5**.

Interestingly, the shortest Eu–N bond is Eu–N(2): 2.543(4) Å presumably as a consequence either of packing effects or steric hindrance of the tetradentate ligand, while the longest one is

Eu(1)–N(3): 2.584(5) Å [being N(2) an sp^3 nitrogen and the pyridinic N(3) an sp^2 nitrogen, respectively]. This behavior is in contrast with the general trend, predicting that the metal–N(sp^2) bond is shorter than metal–N(sp^3) one, as observed by Gregolinski et al. [22] who presented a study of the crystal structures of some rare earth ion complexes with ligands very similar to our tetradentate molecules. Interestingly, the disordered nitrate ions with the N5 nitrogen atom are differently bound to the europium ion in the two conformational isomers. In particular, while in the minor species the nitrate is weakly bonded [i.e. Eu(1)–O(1b) 2.60(2) Å and Eu(1)–O(2b) 2.624(5) Å] in a bidentate coordination mode, in the major one it is more strongly connected but in an asymmetric coordination mode [i.e. Eu(1)–O(1a) 2.644(4) Å and Eu(1)–O(2a) 2.506(8) Å].

Finally, a close inspection of the crystal packing reveals the presence of intermolecular N–H···O hydrogen bonds running in a direction almost parallel to the crystallographic *b* axis. These hydrogen bonds of moderate strength, involving the amine hydrogens and nitrate oxygens join together the complex molecules, forming parallel chains (Fig. 6).

A close inspection of the Eu–O and Eu–N bond lengths as well as of the N–Eu–N bite angles for complex **5** and the dominant conformer of complex **6**, reveals that for the former the two Eu–N (py) bond lengths are almost identical and the distribution of both the Eu–O bond lengths and N–Eu–N bite angles fall in a narrower range (Table 2). Also in the case of the minor conformer observed in the crystal of complex **6** we observe a narrower range of Eu–O bond lengths than that in the main conformer. From these evidences we can conclude that the more distorted (less symmetric) environment around the Eu(III) ion was observed in the main conformer of complex **6**. This fact is in agreement with the major conformational flexibility of the amine ligand **2** that generates a less symmetric (or more distorted) coordination environment.

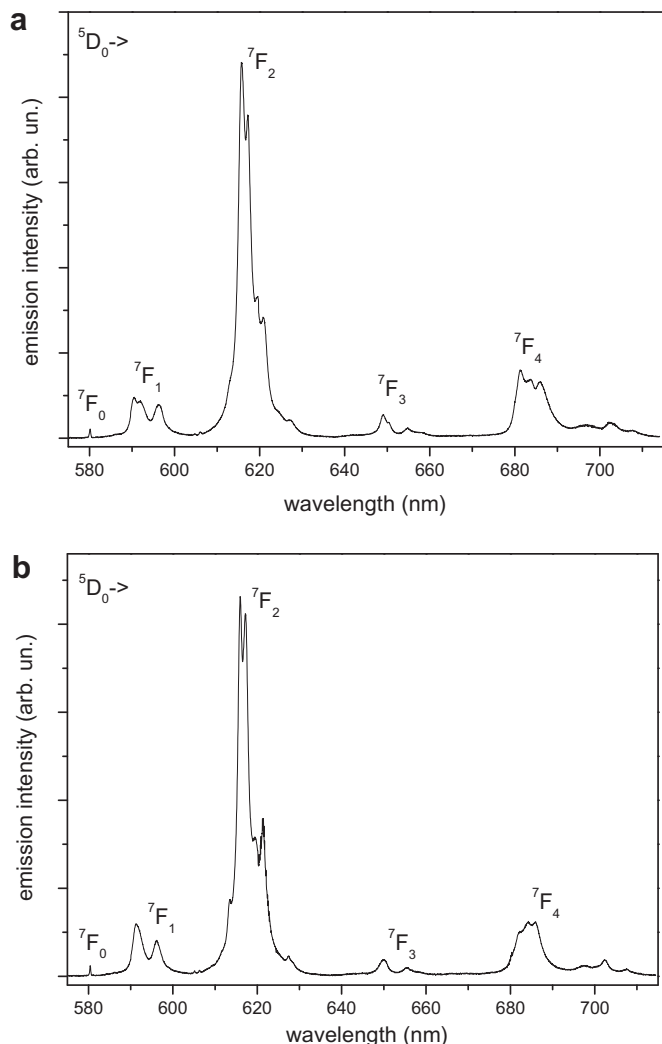


Fig. 7. (a) Emission spectrum of the complex **5** $\lambda_{exc} = 465$ nm and (b) emission spectrum of the complex **7** $\lambda_{exc} = 465$ nm.

3.2. Optical spectroscopy

The room temperature luminescence spectra of the complexes containing the imine ligands, obtained upon excitation at 465 nm (i.e. in the 5D_2 level) are shown in Fig. 7. The spectra are very similar and show the typical profile of the emission from the 5D_0 level of the Eu(III) ion in a strongly distorted environment, with a dominant $^5D_0 \rightarrow ^7F_2$ hypersensitive band. The Stark splittings of the terminal 7F_j ($j = 1-4$) levels are not fully resolved and therefore are not informative. However, the relative intensity of the $^5D_0 \rightarrow ^7F_0$ (briefly, 0–0) band is extremely low, indicating that the effective local symmetry at the metal ion is not strongly axial.

On the other hand, the emission spectra of the complexes containing the amine ligands are characterized by different features (Fig. 8). In fact, they present again a dominant hypersensitive transition, characteristic of generally low symmetry at the Eu(III) ion, but in both cases the 0–0 band is far stronger than for the complexes discussed above. This indicates that the symmetry around the metal ion is lower, and is compatible of an axial character typical of the C_n and C_{nv} point groups which have been shown to give rise to strong 0–0 transitions [23,24]. This feature seems to be detectable from the crystal structures of the compound **6**. The lower effective local symmetry at the Eu(III) ion, according to the luminescence spectra, for the complexes (**6**) and (**8**) can be explained

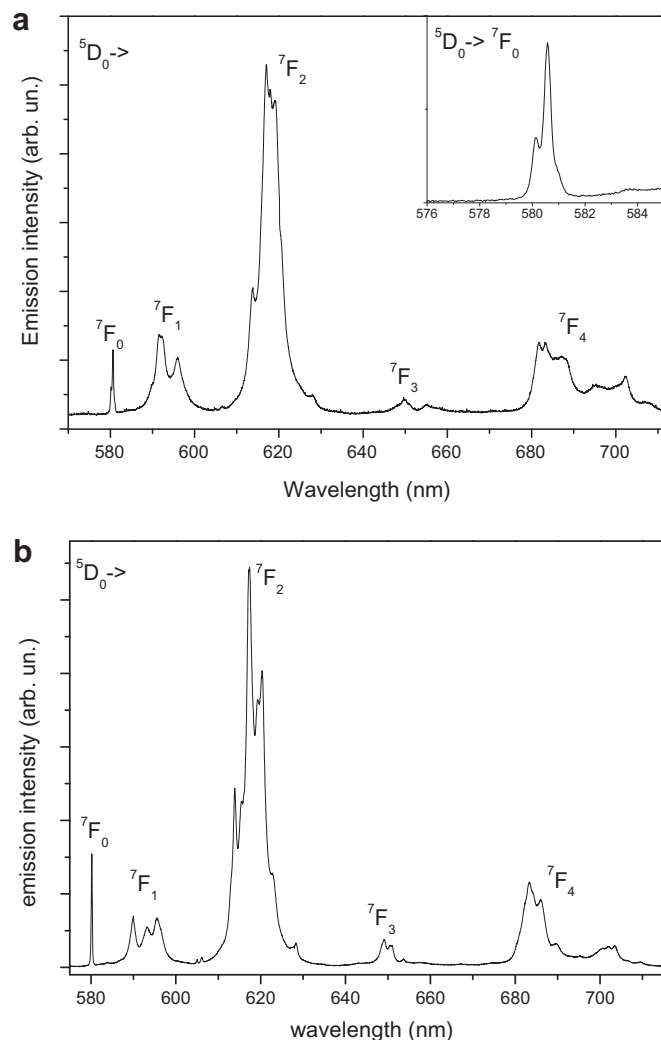


Fig. 8. (a) Emission spectrum of the complex **6** $\lambda_{exc} = 465$ nm and (b) emission spectrum of the complex **8** $\lambda_{exc} = 465$ nm.

taking into account the higher flexibility of the amine ligands compared to the imine ones, allowing for a possible stronger distortion of the first coordination sphere of Eu(III). We also note that for complex (**6**) two features are present in the region of the 0–0 transition, therefore indicating the presence of two Eu(III) emitting centres (see inset of Fig. 8a).

This observation is consistent with the presence of disorder in the nitrate ligands, giving rise to two different conformational isomers in the crystal structure (see above).

The room temperature decay curves of the 5D_0 level of Eu(III) in the various complexes are almost perfectly exponential, as shown in the Fig. 9, even in the case of complex **6** where two emitting conformational isomers, characterized by different coordination environment for Eu(III) ion, are present. Presumably, these two species possess very similar decay kinetics of the 5D_0 level yielding no detectable deviations from a single exponential decay. The lifetimes of the emitting level extracted from the experimental curves are reported in Table 3, whose inspection clearly shows a large difference between the imine and amine complexes. In the former case, the lifetimes are close to 1 ms, therefore indicating that multiphonon relaxation due to high frequency vibrations is not operative, as expected from the absence of N–H groups in the organic ligand. On the other hand, for complexes (**6**) and (**8**) containing

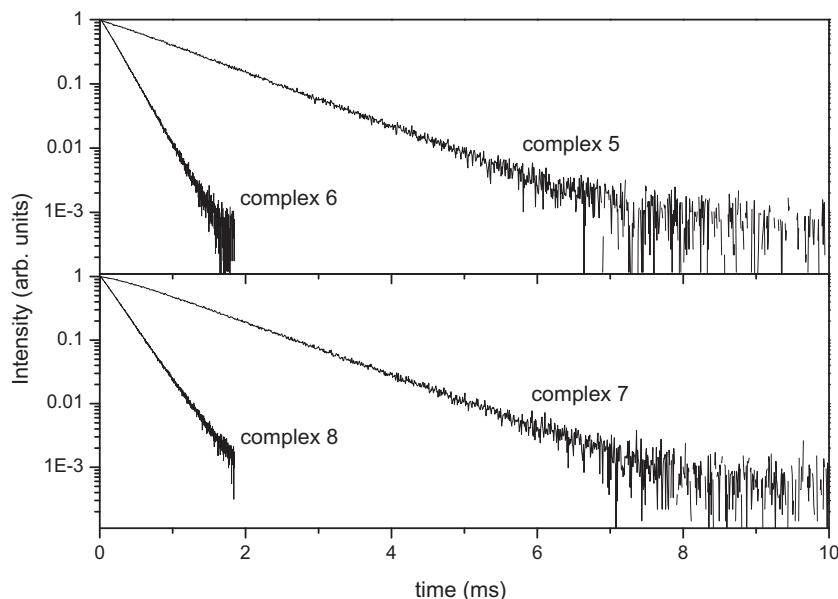


Fig. 9. Decay curves of 5–8 complexes.

Table 3

5D_0 lifetime (τ_{obs}) of the complexes under investigation.

Crystalline compound	5D_0 excited state τ_{obs} (ms)
5	0.94(1)
6	0.22(1)
7	1.07(1)
8	0.26(1)

an amine ligand, the presence of two N–H amino groups in close proximity to the metal ion induces the presence of a non-radiative relaxation mechanism resulting in short lifetimes just above 0.2 ms.

In the case of amine complexes the lifetimes were measured also at 77 K and they were found to be equal to the ones recorded at room temperature. Since the N–H multiphonon relaxation process is known to be in practice temperature independent, it appears to be the only active non-radiative relaxation channel.

Finally, the high affinity for the nitrate ion of these new family of pyridine-based Eu(III) moieties could be exploited in order to detect the presence of NO_3^- in solution. In fact, molecules similar to 5–8 complexes, containing a weak coordinating anion instead of nitrate can be easily prepared. The anion substitution in the first coordination sphere of the weakly coordinating anion with nitrate, should experience a change of the geometrical environment and therefore of the spectroscopic behavior of the Eu(III) ion. The same idea could be successfully applied in order to detect chiral molecules, such as biological substrates.

4. Conclusions

In the present paper we presented an easy synthetic protocol, free from time-consuming purification procedures, which allows obtaining in a high chemical yield a new family of pyridine-based chiral ligands and their chiral nitrate Eu(III) complexes. From structural and spectroscopic evidences in the solid state, we observed an Eu(III) ion environment characterized by low symmetry for all the complexes. However, the lower $^5D_0 \rightarrow ^7F_0$ Eu(III) emission intensity observed in the case of the imine-based complexes reflects a less distorted metal surroundings due to the more conformationally rigid imine ligands 1 and 3. The configuration of

the stereogenic carbons on the cyclohexyl backbone seems to marginally affect the spectroscopic features of the Eu(III) ion emission in the case of imine-based complexes, while for the amine-based complexes the high intensity of the $^5D_0 \rightarrow ^7F_0$ Eu(III) emission probably indicates a more axially distorted crystal field around the metal ion. In addition, due to the high affinity for the nitrate ion of these new chiral pyridine-based Eu(III) moiety, some experiments concerning the luminescence sensing of nitrate anion in solution are currently in progress. Finally, we believe that this new family of chiral Eu(III) complexes can be promising candidates also for the sensing in solution of chiral substrates.

Acknowledgments

The authors gratefully thank Erica Viviani for expert technical. M.M. wish to thank the University of Bologna for financial support.

Appendix A. Supplementary material

CCDC 837304 and 837305 contain the supplementary crystallographic data for this paper. These data can be obtained free of charge from The Cambridge Crystallographic Data Centre via www.ccdc.cam.ac.uk/data_request/cif. Supplementary data associated with this article can be found, in the online version, at [doi:10.1016/j.ica.2011.12.042](https://doi.org/10.1016/j.ica.2011.12.042).

References

- [1] J.-C.G. Bünzli, C. Piguet, *Chem. Soc. Rev.* 34 (2005) 1048.
- [2] M. Albin, W.de W. Horrocks Jr., *Inorg. Chem.* 24 (1985) 895.
- [3] G.R. Choppin, D.R. Peterman, *Coord. Chem. Rev.* 174 (1998) 283.
- [4] M. Albin, R.R. Whittle, W.de W. Horrocks Jr., *Inorg. Chem.* 24 (1985) 4591.
- [5] J.-C.G. Bünzli, *Chem. Rev.* 110 (2010) 2729.
- [6] G. Muller, *Dalton Trans.* (2009) 9692.
- [7] P. Gawryszewska, J. Legendziewicz, Z. Ciunik, N. Esfandiari, G. Muller, C. Piguet, M. Cantuel, J.P. Riehl, *Chirality* 18 (6) (2006) 406.
- [8] B.S. Murray, D. Parker, C.M.G. dos Santos, R.D. Peacock, *Eur. J. Inorg. Chem.* (2010) 2663.
- [9] H.C. Aspinall, *Chem. Rev.* 2002 (1807) 102.
- [10] T. Yamada, S. Shinoda, H. Tsukube, *Chem. Commun.* (2002) 1218.
- [11] J. Lisowski, S. Ripoli, L. Di Bari, *Inorg. Chem.* 43 (2004) 1388.
- [12] S.C.J. Meskers, H.P.J.M. Dekkers, *J. Phys. Chem. A* 105 (2001) 4589.
- [13] G.-L. Law, C. Man, D. Parker, J.W. Walton, *Chem. Commun.* 46 (2010) 2391.

- [14] C.P. Montgomery, E.J. New, D. Parker, R.D. Peacock, *Chem. Commun.* (2008) 4261.
- [15] S. Kano, H. Nakano, M. Kojima, N. Baba, K. Nakajima, *Inorg. Chim. Acta* 349 (2003) 6.
- [16] SMART & SAINT Software Reference Manuals, version 5.051 (Windows NT Version), Bruker Analytical X-ray Instruments Inc., Madison, WI, 1998.
- [17] G.M. Sheldrick, SADABS, program for empirical absorption correction, University of Göttingen, Germany, 1996.
- [18] A. Altomare, M.C. Burla, M. Camalli, G.L. Cascarano, C. Giacovazzo, A. Guagliardi, A.G.G. Moliterni, G. Polidori, R. Spagna, *J. Appl. Crystallogr.* 32 (1999) 115.
- [19] G.M. Sheldrick, SHELXTLplus (Windows NT Version) Structure Determination Package; Version 5.1, Bruker Analytical X-ray Instruments Inc., Madison, WI, USA, 1998.
- [20] E. Keller, SCHAKAL A Computer Program for the Graphic Representation of Molecular and Crystallographic Models, Institute for Crystallography of the University of Freiburg, Freiburg (Germany), 1997.
- [21] N.G. Connelly, T. Damhus, R.M. Hartshorn, A.T. Hutton, IUPAC. Nomenclature of Inorganic Chemistry, Recommendations 2005, RSC Publishing, Cambridge, 2005.
- [22] J. Gregolinski, P. Starynowicz, K.T. Hua, J.L. Lunkley, G. Muller, J. Lisowski, *J. Am. Chem. Soc.* 130 (2008) 17761.
- [23] B. Piriou, D. Falimi, J. Dexpert-Ghys, A. Taitai, J.L. Lacout, *J. Lumin.* 39 (1987) 97.
- [24] R.D. Peacock, *Struct. Bond.* 22 (1975) 83.